Molecular Therapy
Nucleic Acids
Original Article

mRNA-based therapy in a rabbit model of variegate porphyria offers new insights into the pathogenesis of acute attacks

Daniel Jericó,[1,2] Karol M. Córdoba,[1,2] Lei Jiang,[3] Caroline Schmitt,[4,5] María Morán,[6,7] Ana Sampedro,[1,2] Manuel Alegre,[2,8] María Collantes,[2,9,10] Eva Santamaría,[1,2] Estíbaliz Alegre,[2,11] Corinne Culerier,[4,5] Ander Estella-Hermoso de Mendoza,[12] Julen Oyarzabal,[12] Miguel A. Martín,[6,7] Iván Peñuelas,[2,9,10] Matías A. Ávila,[1,2,13] Laurent Gouya,[4,5] Paolo G.V. Martini,[3,14] and Antonio Fontanellas[1,2,13,14]

[1]Hepatology Program, Centre for Applied Medical Research (CIMA), University of Navarra, 31008 Pamplona, Spain; [2]Instituto de Investigación Sanitaria de Navarra (IdiSNA), 31008 Pamplona, Spain; [3]Moderna Inc., Cambridge, MA 02139, USA; [4]Centre de Recherche sur l'Inflammation, Institut National de la Santé et de la Recherche Médicale U1149, 75018 Paris, France; [5]Centre Français des Porphyries, Hôpital Louis Mourier, Assistance Publique-Hôpitaux de Paris, Colombes et Université de Paris, 92701 Colombes, France; [6]Mitochondrial Diseases Laboratory, Instituto de Investigación Sanitaria Hospital 12 de Octubre (imas12), 28041 Madrid, Spain; [7]Centro de Investigación Biomédica en Red de Enfermedades Raras (CIBERER), U723, Instituto de Salud Carlos III, 28029 Madrid, Spain; [8]Department of Clinical Neurophysiology, Clínica Universidad de Navarra (CUN), 31008 Pamplona, Spain; [9]MicroPET Research Unit, CIMA-CUN, 31008 Pamplona, Spain; [10]Nuclear Medicine Department, CUN, 31008 Pamplona, Spain; [11]Department of Biochemistry, Service of Biochemistry, Clínica Universidad de Navarra (CUN), 31008 Pamplona, Spain; [12]Small Molecule Discovery Platform, Molecular Therapeutics Program, CIMA-University of Navarra, 31008 Pamplona, Spain; [13]Centro de Investigación Biomédica en Red de Enfermedades Hepáticas y Digestivas (CIBEREHD), Instituto de Salud Carlos III, 28029 Madrid, Spain

Variegate porphyria (VP) results from haploinsufficiency of protoporphyrinogen oxidase (PPOX), the seventh enzyme in the heme synthesis pathway. There is no VP model that recapitulates the clinical manifestations of acute attacks. Combined administrations of 2-allyl-2-isopropylacetamide and rifampicin in rabbits halved hepatic PPOX activity, resulting in increased accumulation of a potentially neurotoxic heme precursor, lipid peroxidation, inflammation, and hepatocyte cytoplasmic stress. Rabbits also showed hypertension, motor impairment, reduced activity of critical mitochondrial hemoprotein functions, and altered glucose homeostasis. Hemin treatment only resulted in a slight drop in heme precursor accumulation but further increased hepatic heme catabolism, inflammation, and cytoplasmic stress. Hemin replenishment did protect against hypertension, but it failed to restore action potentials in the sciatic nerve or glucose homeostasis. Systemic porphobilinogen deaminase (PBGD) mRNA administration increased hepatic PBGD activity, the third enzyme of the pathway, and rapidly normalized serum and urine porphyrin precursor levels. All features studied were improved, including those related to critical hemoprotein functions. In conclusion, the VP model recapitulates the biochemical characteristics and some clinical manifestations associated with severe acute attacks in humans. Systemic PBGD mRNA provided successful protection against the acute attack, indicating that PBGD, and not PPOX, was the critical enzyme for hepatic heme synthesis in VP rabbits.

INTRODUCTION

Porphyrias are a group of rare diseases caused by a deficiency in one of the eight enzymes of the heme biosynthesis pathway. Based on their clinical features porphyrias are classified into three types: cutaneous, acute, or mixed.[1–3] Variegate porphyria (VP, MIM:176200) is classified as a mixed porphyria due to the accumulation of both porphyrins and porphyrin precursors. It is an autosomal dominant metabolic disease that results from deficiency of protoporphyrinogen oxidase (PPOX, EC 1.3.3.4), the seventh enzyme of the heme pathway. As a consequence, there is hepatic accumulation of protoporphyrinogen, the substrate of PPOX. This, as well as other heterocyclic porphyrins, undergoes chemical oxidation, which is related to the phototoxic lesions affecting sunlight-exposed areas of the skin. VP is also characterized by the accumulation of porphyrin precursors, δ-aminolevulinic acid (ALA), and porphobilinogen (PBG), which are associated with the neurovisceral acute attacks of porphyria.[4] However, the relationship between high ALA and PBG levels and the prodrome is still unclear.

Acute neurovisceral attacks involve abdominal pain, nausea, vomiting, and hypertension, among other nonspecific symptoms. Peripheral neuropathy can be manifested as paresis in the upper and lower

Received 12 December 2020; accepted 13 May 2021;
https://doi.org/10.1016/j.omtn.2021.05.010.

[14]These authors contributed equally

Correspondence: Paolo G.V. Martini, Moderna Inc., 200 Technology Square, Cambridge, MA 02139, USA.
E-mail: paolo.martini@modernatx.com
Correspondence: Antonio Fontanellas, Hepatology Program, Centre for Applied Medical Research (CIMA), University of Navarra, 55 Avenida Pío XII, 31008 Pamplona, Spain.
E-mail: afontanellas@unav.es

extremities. Central nervous system involvement (seizures, insomnia, anxiety, confusion, and depression) can also be present during an acute attack.[1,5] Porphyria attacks can be triggered by exogenous (such us medications/chemicals, excess alcohol intake, smoking, infection) or endogenous (steroid hormones, stress, or fasting) factors that strongly induce the expression of ALA synthase (ALAS, EC 2.3.1.37).[1,2] ALAS1 is the first and rate-limiting enzyme of the pathway in the liver and can be upregulated after the administration of certain drugs,[6] or during starvation via the peroxisome proliferator-activated receptor γ co-activator 1α (PGC1α).[7] Additional regulation of ALAS1 occurs with the negative feedback mechanism of heme caused by increased demand for hepatic hemoproteins or degradation through induction of heme oxygenase-1 (HO-1) gene (EC 1.14.14.18).[8,9] Furthermore, heme also decreases the stability of *ALAS1* mRNA,[10] inhibits uptake of pre-ALAS1 into the mitochondria,[11] and reduces the stability of the mitochondrial ALAS1 protein via Lon peptidase 1-mediated degradation.[12]

Current treatment of acute attacks relies on i.v. hemin infusion, which restores the hepatic heme pool, thereby initiating the inhibitory feedback mechanism to hepatic ALAS1 and thus reduces heme precursor production and excretion.[13] Recently, givosiran, an RNA interference agent targeting hepatic *ALAS1*, has received US Food and Drug Administration (FDA) approval for the prevention of recurrent porphyric attacks in severely affected patients.[14,15] Liver transplantation has been proven to cure the disease,[16] suggesting that liver is the major etiologic site of the disease and thus a primary target for a therapeutic agent.[17]

A mouse model of VP ($R59W^{+/-}$ mice) has been developed and recapitulates porphyrin accumulation in a pattern similar to that in human VP patients.[18] However, this model fails to recapitulate ALA and PBG accumulation and the clinical manifestations associated with an acute attack.

The aim of this study was to characterize from a biochemical and clinical perspective a novel model of chemically induced porphyrin precursor accumulation in rabbits. Previous work reported that administration of 2-allyl-2-isopropylacetamide (AIA) in female New Zealand rabbits caused a moderate accumulation of porphyrin precursors.[19] However, it did not reproduce the clinical features associated with acute attacks, and both urinary ALA and PBG levels spontaneously normalized a few hours after drug administration. In an attempt to extend ALA and PBG accumulation and reproduce the clinical symptoms of the porphyric acute attacks, we administered the antibiotic rifampicin together with AIA to synergistically increase heme demand and decrease PPOX activity, as previously reported in healthy volunteers.[20] Finally, we evaluated the therapeutic efficacy against acute attacks of the administration of hemin, the common treatment in acute porphyrias, and of a human PBG deaminase (hPBGD) mRNA delivered in lipid nanoparticles (LNPs). Systemic administration of hPBGD mRNA has been shown to quickly increase hepatic PBGD activity and effectively normalize ALA and PBG accumulation in a mouse model of PBGD deficiency,[21] and in the present study we demonstrate its effectiveness in preventing acute attacks in a rabbit model of porphyria.

RESULTS

Biochemical characterization of a novel rabbit model of VP

Repeated administrations of AIA and rifampicin in rabbits during 20 days halved PPOX activity (Figure 1A) and strongly induced *Alas1* and *Ho-1* gene expression in the liver (Figures 1B and 1C) and increased ALAS1 protein level, as measured by immunoblot (Figure S1A). As a consequence, total urinary excretion of heme precursors on the last day of the study increased by 80-fold in challenged rabbits when expressed as moles of ALA (2 mol of ALA are required to form 1 mol of PBG and 8 mol of ALA form one porphyrin) (Figure 1D). High levels of urinary PBG (Figures 1E and 1F) and porphyrins (Figures 1G, 1H, and S1B) were measured throughout the study. No significant increase of urinary ALA levels (Figures 1F and S1C) occurred until the third challenge (days 15–19 [D15]), which was the longest (5 days of challenge). Porphyrin precursor determination in cerebrospinal fluid extracted on day 20 did not show ALA accumulation (<0.05 μM), but high PBG levels were detected in two rabbits treated with AIA and rifampicin (0.47 ± 0.28 μM versus <0.05 μM in control rabbits, n = 2). Thus, the accumulation of the ALA metabolite requires an extended induction of the heme synthesis pathway in this model.

While recurrent co-administration of AIA and rifampicin induced both gene expression and activity of the hepatic ALAD enzyme (Figure S2B, left and right panels, respectively), the other cytoplasmic enzymes of the pathway, that is, PBGD, UROS, and UROD (Figure S2A), remained unchanged (Figures 1I and S2C–S2E). Enzymatic ALAD activity was increased nearly 3-fold in the VP rabbits compared with non-injected animals. This may explain the higher PBG/ALA ratio in the urine samples of VP rabbits (Figure 1F).

A significant inhibition was observed in the activity of the three mitochondrial enzymes, that is, CPOX, PPOX, and FECH (Figures S2F–S2H, right panels). However, the expression of their respective genes was repressed, unchanged, and induced, respectively (Figures S2F–S2H, left panels). These data suggest that metabolites derived from AIA and rifampicin directly interfere with the activity of the last three enzymes of the pathway, mainly PPOX.

Highly carboxylated porphyrins, that is, the octocarboxylated uroporphyrin and heptacarboxylporphyrin fractions, predominated when compared to tetracarboxylated coproporphyrin and pentacarboxylporphyrin (Figure 1G). Plasma porphyrin levels were also very high (Figure 1H), with a specific plasma fluorometric emission maximum around 622–623 nm for most of the samples. In VP patients, plasma fluorescence emission maximum wavelengths are characteristically between 624 and 627 nm, whereas they are around 618–620 nm in acute intermittent porphyria (AIP, MIM: 17600) patients.[1,22] After plasma protein precipitation in samples from two animals challenged with AIA and rifampicin, porphyrin concentrations dropped by a half (from 2,276 ± 234 nmol/L total porphyrin to 1,057 ± 59 nmol/L free porphyrin), which suggests a major accumulation of protoporphyrinogen bound to proteins.

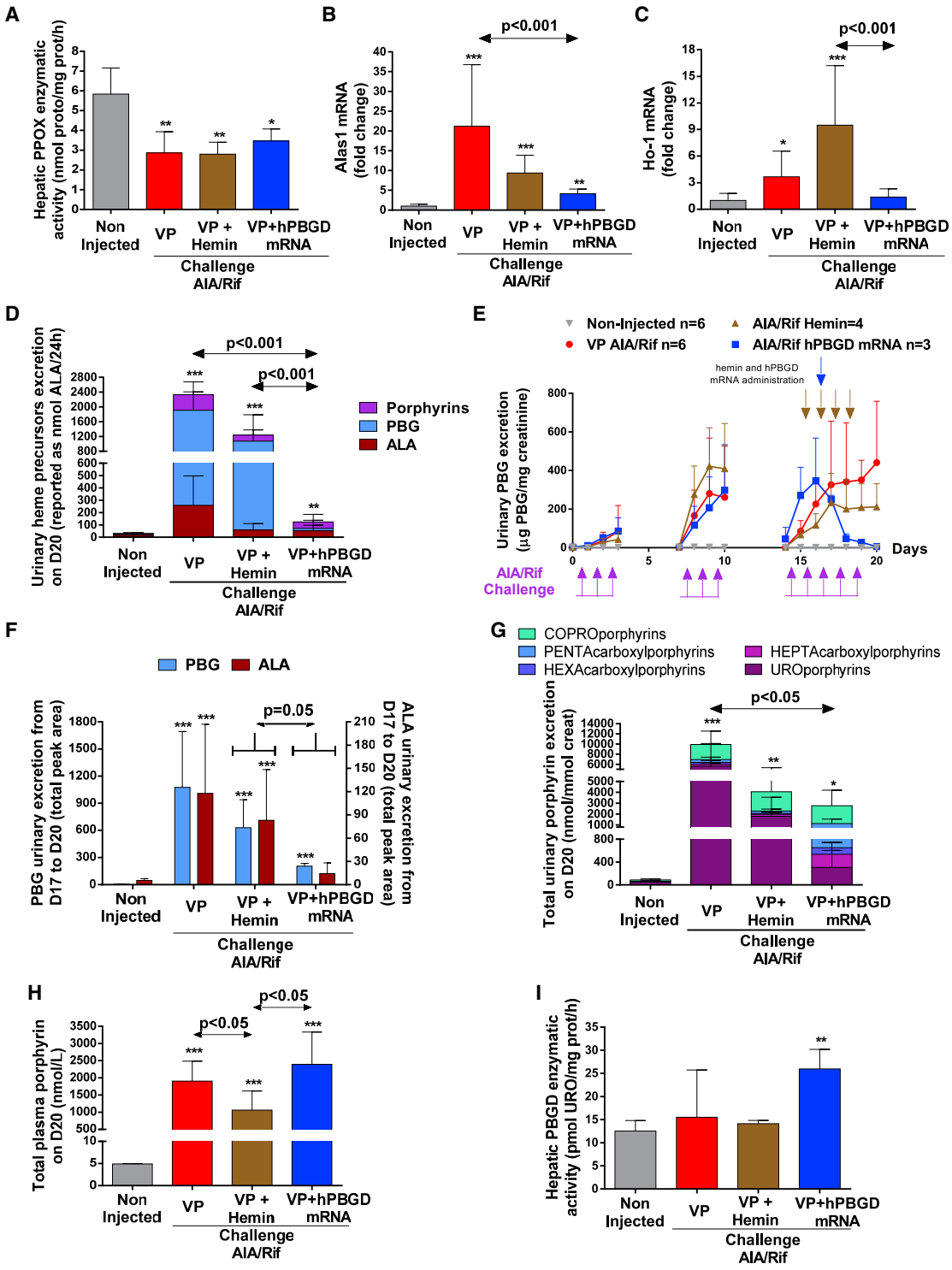

Figure 1. Biochemical characterization of the variegate porphyria model in rabbits and the effects of common and emerging therapies for acute attacks, hemin, and hPBGD mRNA, respectively

Eleven doses of AIA (350 mg/kg, s.c.) and twelve doses of rifampicin (200 mg/kg, i.p.) were administered to 13 female New Zealand rabbits during 20 days. Of these, hemin (8 mg/kg) was i.p. injected into four animals on days 15–18 (brown arrows) and hPBGD mRNA (0.5 mg/kg) was i.v. administered on day 16 (blue arrow) in another three rabbits. Seven un-injected rabbits were used as a reference group. (A) PPOX activity and the expression of the two regulatory enzymes of heme metabolism and catabolism,

(legend continued on next page)

Finally, repeated administration of AIA and rifampicin increased fecal porphyrin excretion (132 ± 74 nmol/g, n = 2; normal values <30 nmol/g). Fecal porphyrin fractionation showed a major peak of dicarboxylic protoporphyrin (84% protoporphyrin, 2.6% harderoporphyrin, 7.9% coproporphyrin, 1.5% isocoprophyrin, 3.0% pentaporphyrin, 0.2% hexaporphyrin, 0.1% heptaporphyrin, and 0.6% uroporphyrin) (Figure S3). Tetracarboxylic coproporphyrin can be excreted in both urine and feces. Preferential urinary excretion of the coproporphyrin in this model (31.6% ± 16.8% in urine versus 9.4% ± 4% in feces, $p < 0.03$) may be due to energy metabolism saving compared to the biliary secretion, which is energetically more expensive. All of these results suggest that this model recapitulates the biochemical characteristics of VP.

Effects of hemin and hPBGD mRNA administration on heme precursor accumulation

The administration of four doses of hemin, the current standard of care for acute attacks in humans, only showed a slight reduction in hepatic *Alas1* gene expression (Figure 1B) and protein level (Figure S1A), but further increased *Ho-1* expression (Figure 1C). For the rest of the enzymes of the heme synthesis, their hepatic activity was not modified after hemin or hPBGD mRNA treatment although their expression increased after hemin administration (Figure S2). As a result of the hemin treatment, the urinary excretion of porphyrin precursors (Figures 1D–1F and S1C) and porphyrins (Figures 1G and S1B), as well as plasma porphyrin levels (Figure 1H), were only slightly reduced.

Although this model showed significant PBG accumulation, recurrent challenges with AIA and rifampicin did not modify hepatic PBGD activity (Figure 1I). Of note, the administration of a single dose of hPBGD mRNA on day 16 (D15 challenge) increased hepatic PBGD activity 2-fold, as measured on day 20 (Figure 1I). As a result, PBG excretion was normalized (Figures 1E and 1F), and the increase in urinary ALA excretion that occurred in the VP group on day 17 was not observed (Figure S1C). The administration of hPBGD mRNA increased urinary porphyrin levels during the 2 days post-injection (Figure S1B). This is likely due to the monopyrrole PBG being rapidly metabolized by exogenous PBGD to form tetrapyrrole porphyrins. On day 20, 4 days after hPBGD mRNA administration, the liver of treated rabbits showed normal expression levels of the key regulatory enzymes of heme synthesis (*Alas1*, Figure 1B) and catabolism (*Ho-1*, Figure 1C), which correlated with the normal urinary excretion of heme precursors observed (Figure 1D).

In a separate acute treatment study, hPBGD mRNA was administered when high urinary concentrations of both PBG and ALA were observed. The administration of a single hPBGD mRNA dose (0.5 mg/kg, intravenously [i.v.]) significantly reduced serum accumulation of PBG (Figure S4A) and ALA (Figure S4B) within 8 h, and rabbits recovered normal serum levels of these two precursors by 22 h post-injection.

Liver status and functionality of hepatic hemoproteins

The liver of VP rabbits showed normal weight (93.9 ± 5.3 g versus 88.2 ± 7.3 g in the control group) and normal histology as stained by hematoxylin and eosin (data not shown). Regarding liver status, serum alkaline phosphatase (ALP) levels were normal (Figure 2A), while a slight increase in liver alanine aminotransferase (ALT) was observed on day 20 (Figure 2B). Of interest, liver tissue immunostaining for mitochondrial cytochrome *c* oxidase 1 (MT-CO1 of the respiratory complex IV) protein showed an abnormal distribution on the periphery of hepatocytes (Figure S5).

Mitochondrial energy metabolism was examined in mitochondria isolated from the liver of VP rabbits by determining the activity of the mitochondrial oxidative phosphorylation (OXPHOS) complexes I–IV and the analysis of the complex protein levels, using an OXPHOS antibody cocktail. The activities were measured at the maximum enzymatic rate with saturation of substrates and were therefore independent of the contribution of the tricarboxylic acid (TCA) cycle. Our results suggest that mitochondrial complex I, II, III, and IV enzyme activities are markedly reduced in VP rabbits (Figures S6A–S6D and 2C), although only the protein levels of complex IV, measured by MT-CO1 immunoblot, showed a significant decrease (Figures 2D and S6E).

Of note, complex IV contains heme *a*, whereas complex II has type *b*, and both heme *b* and *c* are present in complex III. Type *b* and *c* are similar to protoheme and they are not chemically modified before assimilation into the corresponding apoprotein. In contrast, heme *a* needs further modifications by addition of farnesyl and formyl groups to protoheme.[23] In the VP rabbits, the administration of AIA and rifampicin greatly increased hepatic heme (Figure 2E) and mitochondrial hepatic heme *a* (Figure 2F) levels. Of interest, animals that received hPBGD mRNA further increased heme *a* levels (Figure 2F), displayed normal complex IV protein levels (Figure 2D), and partially reversed the activity deficiency of the four mitochondrial complexes (Figures S6A–S6D and 2C). Hemin (ferric chloride heme) administration failed to normalize either the amount of protein in complex IV (Figure 2D) or the activity of complexes I–IV (Figures S6A–S6D and 2C).

Dysregulation of the mitochondrial respiratory chain and a high accumulation of porphyrin precursors are related to the induction of oxidative stress. The expression of the hepatic *Hepcidin* gene, a

(B) *Alas1* and (C) *Ho*-1, respectively, were measured in liver samples 16 h after the last rifampicin administration. Rabbits were housed in individual cages, and 24-h urine samples were collected during challenges. (D) Total urinary loss of heme precursors on day 20 reported as nmol ALA per 24 h (two ALA molecules are required to synthesize a PBG monopyrrole, and eight ALA molecules are required to synthesize one porphyrin). (E) Urinary PBG excretion over time. (F) Quantification of the total peak area of the urinary PBG and ALA excretion between days 17 and 20. (G) Urinary excretion of individual porphyrins and (H) total plasma porphyrin levels on day 20. (I) Hepatic PBGD activity measured at sacrifice. Data are means ± SD. *$p < 0.05$, **$p < 0.01$, ***$p < 0.001$ against the non-injected group. VP, variegate porphyria; AIA, allyl-2-isopropylacetamide; rif, rifampicin; PPOX, protoporphyrinogen oxidase; ALA, δ-aminolevulinic acid; ALAS1, ALA-synthase 1; PBG, porphobilinogen.

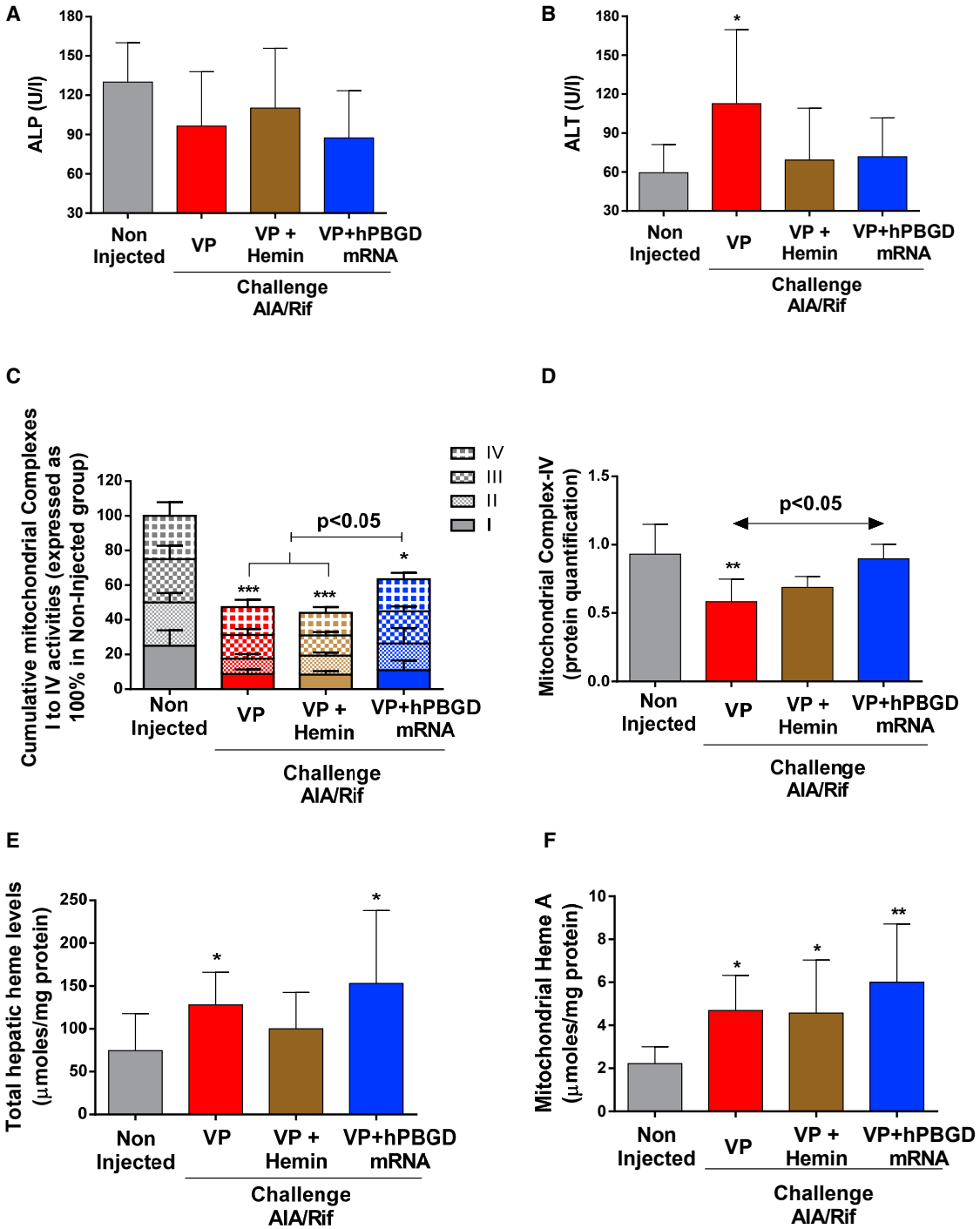

Figure 2. Liver status and function in rabbits challenged with AIA and rifampicin (n = 6) and the effects of the administration of hemin (n = 4) and hPBGD mRNA (n = 3)

Serum (A) ALP and (B) ALT levels from cardiac-puncture blood samples taken at sacrifice (day 20). (C) Cumulative activity of the mitochondrial respiratory complexes I–IV. (D) Mitochondrial complex IV content as quantified by western blot from liver samples. (E) Total heme and (F) mitochondrial heme *a* content measured in liver samples. Control group corresponds to non-injected rabbits (n = 6). Data are means ± SD. *p < 0.05, **p < 0.01, ***p < 0.001 versus the non-injected group.

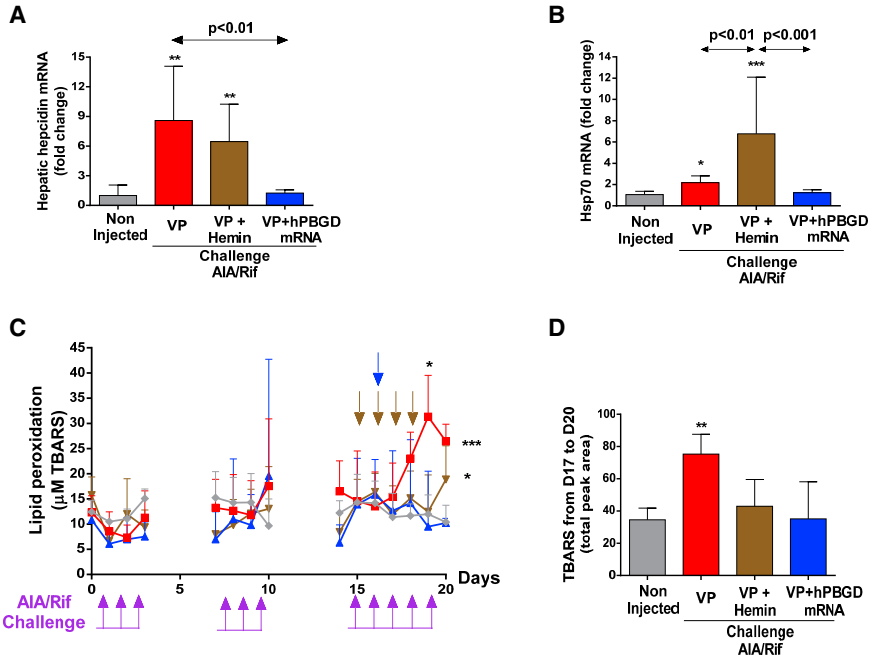

Figure 3. Protective efficacy of a single i.v. administration of hPBGD mRNA on hepatic oxidative stress and inflammation in a chemically induced rabbit model of variegate porphyria

(A and B) Fold change expression levels of (A) *Hepcidin* and (B) *Hsp70* genes determined by qRT-PCR in the rabbits' livers are shown. (C and D) Protective efficacy of hPBGD mRNA against lipid peroxidation was determined by (C) urine TBARS excretion over time and (D) quantification of the total peak area of urinary TBARS levels after treatment with hemin and hPBGD-mRNA (days from 17 to 20). Data are means ± SD. *p < 0.05, **p < 0.01, ***p < 0.001 against the non-injected group.

peptide hormone involved in iron homeostasis and used as a biomarker of oxidative stress and inflammation,[24] was strongly induced in rabbits injected with AIA and rifampicin (Figure 3A). Another biomarker of oxidative stress is the *Hsp70* gene, which was also overexpressed in rabbits challenged with AIA and rifampicin (Figure 3B). Finally, AIA and rifampicin challenges induced a progressive increase of urinary thiobarbituric acid-reactive substance (TBARS) excretion (Figure 3C), a biomarker of lipid peroxidation.[25] It is noteworthy that the highest TBARS values were obtained in the D15 challenge (Figure 3D) concomitant with the rise in ALA excretion (Figure S1C). Urinary excretion of TBARS and ALA showed a remarkably high correlation ($r = 0.914$, $p < 0.001$). The administration of hemin slightly reduced ALA excretion (Figure S1C) and protected against urinary TBARS accumulation (Figures 3C and 3D) but failed to reduce hepatic *Hepcidin* expression (Figure 3A) and further increased the expression of *Hsp70* (Figure 3B). Rabbits treated with hPBGD mRNA showed hepatic *Hepcidin* expression (Figure 3A), *Hsp70* expression (Figure 3B), and urinary TBARS levels (Figures 3C and 3D) within the normal range determined in the non-injected control group.

Clinical characterization of a VP model in rabbits

Systolic blood pressure in rabbits during the days 8–10 (D8) challenge (Figure 4A) was outside the normal range calculated with results obtained from the non-injected group and significantly increased as compared with the corresponding baseline values (Figure 4A). Both hemin and hPBGD mRNA protected these rabbits against hypertension in the D15 challenge (Figure 4B).

Challenge with AIA and rifampicin induced transient motor disturbances as measured by gait difficulties (Video S1) and abnormalities in potential evoked in the sciatic nerve (Figure 4C). Whereas the administration of four doses of hemin only partially protected against gait abnormalities, rabbits injected with a single dose of hPBGD mRNA showed normal gait (Video S2) and amplitude values in the normal range (Figure 4C).

Finally, rabbits challenged with AIA and rifampicin yielded abnormal glucose tolerance test (GTT) results (Figures 4D and 4E) and reduced tissue uptake of glucose after fasting, as measured by biodistribution of the glucose analog ^{18}F-fluorodeoxyglucose (FDG) in positron-emission tomography (PET)/computed tomography (CT) imaging (Figures S7 and S8). Specific quantification of ^{18}F-FDG uptake in the brain (Figure 4F) confirmed significant reduction of glucose uptake in chemically induced fasted rabbits when compared to the non-injected control group (D8 challenge). In the D15 challenge, while hemin treatment failed to protect against these alterations, a single administration of hPBGD mRNA fully normalized GTT, measured by the time at which glucose is cleared from the blood (Figure 4D) and total peak area (Figure 4E) following glucose challenge. hPBGD mRNA also restored brain glucose uptake (Figures 4F and S8).

DISCUSSION

Pharmacological models in large animals are valuable tools to facilitate the translation of experimental therapies from the laboratory to patients.[26] Given that the only murine model described for VP fails to recapitulate the biochemical and clinical manifestations associated with acute attacks, we developed a pharmacological model in rabbits that reproduces the characteristics of acute attacks observed in patients with severe VP.[1–3]

The combined administration of AIA[19] and rifampicin resulted in a strong induction of hepatic heme synthesis, as shown by the rise in ALAS1 gene expression and protein levels, and total hepatic heme levels. These changes may reflect an adaptive response of the hepatocyte to allow metabolism of the injected drugs and/or the inactivation of a heme fraction probably caused by a change in its conformation by the binding of an allyl group.[27,28] AIA has long been known to be a

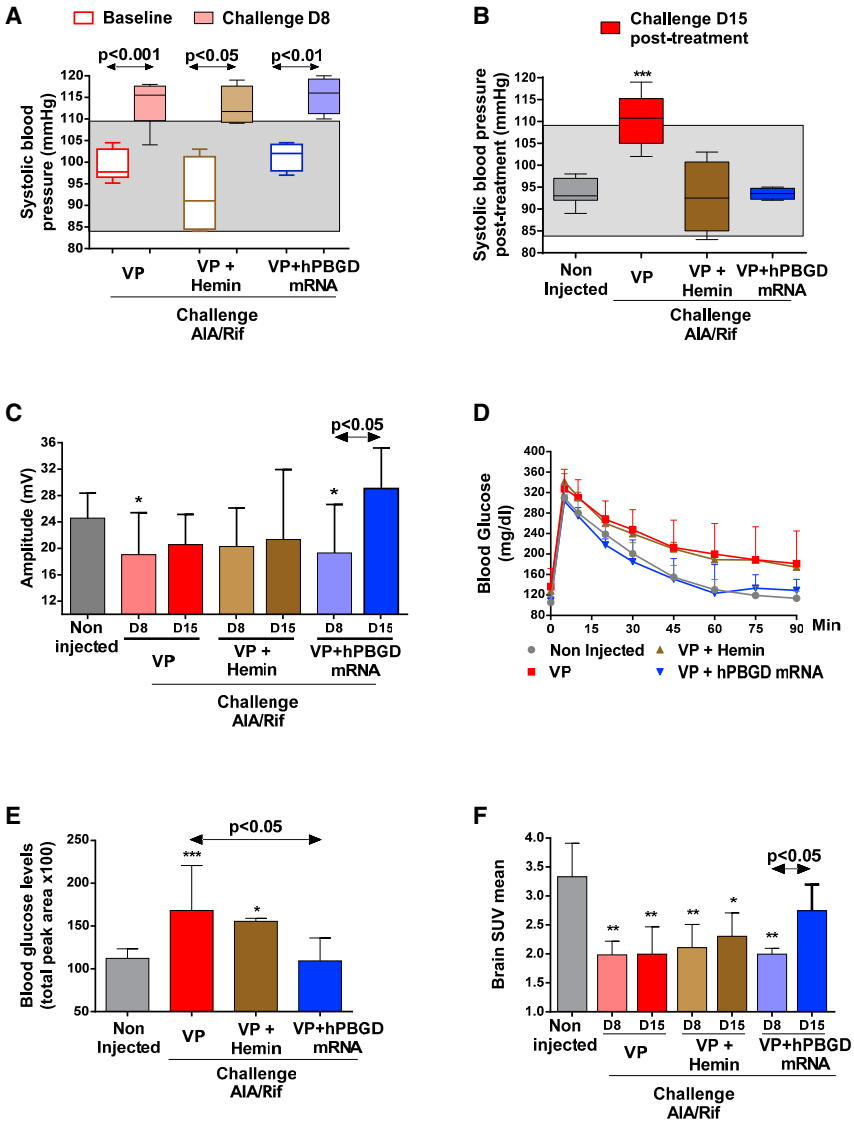

Figure 4. Therapeutic efficacy of a single i.v. administration of hPBGD mRNA in a chemically induced rabbit model of variegate porphyria

(A and B) Systolic blood pressure at (A) baseline (empty boxes) and during the D8 AIA/rifampicin challenge (full boxes) and (B) after treatment during the D15 challenge. Animals treated with hemin or hPBGD-mRNA regained normal systolic blood pressure. (C) Amplitude of sciatic nerve in an electrophysiological nerve conduction velocity study performed at the end of challenges D8 (without treatment) and D15 (which included treatment). (D) A GTT was performed in order to study insulin resistance in fasted rabbits. Serum glucose levels were measured at times 0, 5, 10, 20, 30, 45, 60, 75, and 90 min post-injection of glucose solution (0.5 g/kg, i.v.). (E) Quantification of the total peak area of the serum glucose levels. (F) Brain ^{18}F-FDG uptake in 16-h fasted rabbits performed at the end of challenges D8 (without treatment) and D15 (which included treatment). Data are means ± SD. *p < 0.05; **p < 0.01, ***p < 0.001 versus the non-injected group.

suicide substrate for CYP450s,[29,30] supporting the observation that VP rabbits showed unchanged *Ppox* gene expression but decreased enzyme activity. Our findings agree with a previous report describing reduced leucocyte PPOX activity in seven healthy volunteers after daily administration of rifampicin (600 mg) for a week.[20] Rifampicin together with AIA have been described as strong inducers of CYP3A4 and CYP3A5, and moderate inducers of CYP2B6, CYP2C8, CYP2C9, and CYP2C19,[31–33] thereby further increasing heme demand and inducing hepatic *Alas1* transcription. As a result, VP rabbits showed high porphyrin and porphyrin precursor accumulation, in a pattern similar to patients with VP.[20] Our animals were only exposed to soft light and they did not show any type of skin photosensitivity (data not shown). The accumulation of PBG and ALA is a biochemical hallmark of patients with VP, although the cause is not well known. Some authors suggest potential PBGD inhibition by the low-carboxylated porphyrins.[34] However, VP rabbits treated with hPBGD mRNA showed high concentrations of low-carboxylated porphyrins on days 17 and 18 with no concomitant accumulation of heme precursors. Indeed, the liver of VP rabbits overexpressing hPBGD maintained PPOX inhibition but had decreased the elevated *Alas1* mRNA and protein levels. These data indicate that PBGD is the limiting step of hepatic heme synthesis in these chemically induced VP rabbits.

Moderate and transient changes in liver status could be related to drug administration, as previously reported.[20,35] The hepatic parenchyma was normal, without necrotic areas but exhibiting color changes probably due to the formation of green pigments as previously described.[27–29] A MT-CO1 immunoblot also revealed abnormal mitochondrial distribution on the periphery of hepatocytes. This is probably caused by cytoskeleton restructuring due to an undetermined response to drug administration (see Web resources).

Previous studies have reported disturbances of the redox state and glutathione metabolism in rats administered a large single dose of AIA.[36] The expression of the *Ho-1*, *Hsp70*, and *Hepcidin* genes, all biomarkers of oxidative stress, was strongly induced after recurrent AIA and rifampicin challenges. Of note, while the administration of hPBGD mRNA normalized the expression of these genes, hemin treatment further increased *Ho-1* and *Hsp70* mRNA levels and maintained high *Hepcidin* expression. Although hemin normalized liver transaminases, cytoplasmic stress and inflammation remained higher in the liver of VP rabbits, as similarly reported in AIP mice.[8]

The kinetics of lipid peroxidation throughout the study was determined by measuring urinary TBARS levels. A significant increase in TBARS excretion was observed at the end of the day 15 challenge, which was associated with an increased urinary excretion of ALA. The administration of a single dose of hPBGD mRNA normalized the regulatory steps of the synthesis (*Alas1*) and catabolism (*Ho*-1) of the hepatic heme pathways and fully protected against ALA and TBARS accumulation.

Heme availability for important hemoprotein functions was analyzed in the liver of this rabbit model. Four types of heme are described in eukaryotes, that is, protoheme and heme *a*, *b*, and *c*.[23,37] Protoheme is the precursor of the different types of heme and constitutes a pool of "free heme." The mitochondrial complexes II and III use heme *b*, whereas heme *c* is used by cytochrome *c*1 of complex III, and two groups of heme *a* are part of the MT-CO1 (complex IV). The analysis of complexes I–V protein subunit levels in isolated liver mitochondria showed that the protein content of the MT-CO1 declines after recurrent challenges with AIA and rifampicin, whereas mitochondrial complexes I–III were much less affected. Given that heme *a* needs chemical modifications that differ from *b* and *c*, we hypothesize that the protein content of mitochondrial complex IV is primarily affected under conditions with reduced heme availability.[23] Although hemin administration partially corrected omplex IV heme content, only rabbits treated with hPBGD mRNA showed normal values.

Although the protein content of the mitochondrial respiratory chain complexes I–III remained unchanged in the liver of VP rabbits, their enzymatic activities were markedly reduced. A previous study using a mouse model of AIP also revealed a failure of hepatic mitochondrial energy metabolism and TCA cycle after phenobarbital challenge.[38] Given the close interconnection between TCA and the activity of the respiratory complexes I–III, the authors suggested that the TCA cycle is unable to supply the reduced cofactors to the respiratory chain due to the high demand for succinyl-coenzyme A (CoA) to form ALA. However, in our rabbits, respiratory chain activities were measured independently of the contribution of the TCA cycle. Another difference with this study was that in the AIP mouse model, the activity of the complexes returned to normal after the administration of hemin, but this effect was not seen in our rabbits. We suggest that the high oxidative stress observed in VP rabbits, especially in those treated with hemin, may affect the iron-sulfur clusters that contain complexes I–III. Such clusters containing enzymes are known to represent critical targets for the oxygen free radicals[39] that contribute to the pathophysiology of the acute attack.[40] Of interest, the administration of a single dose of hPBGD mRNA prevented the induction of oxidative stress and tended to normalize the activity of the respiratory complexes.

Recurrent AIA and rifampicin challenges reproduced some of the signs and symptoms associated with the acute attacks of porphyria, such as motor impairment,[41] hypertension,[42] and altered glucose homeostasis.[43] Hypertension is a common symptom in acute porphyrias and was previously described in a PBGD-deficient mouse model during a challenge with phenobarbital.[21] In our rabbits, both hemin and hPBGD mRNA administration protected against hypertension. These data suggest that this parameter is not affected by the accumulation of porphyrins and porphyrin precursors that still persist after hemin replacement therapy.

Motor impairment is also described in severely affected patients with acute porphyrias[41] and mouse models with PBGD deficiency, as measured by the rotarod test, reduced stride length, and decreased amplitude of the action potentials in the compound muscle after phenobarbital-induced attacks.[44,45] While both hemin and hPBGD mRNA administration protected against gait problems in our VP rabbits (Videos S1 and S2), only hPBGD mRNA efficiently restored the compound motor action potential of the sciatic nerve. Thus, the amplitude parameter is probably affected by the accumulation of heme precursors that still persist in hemin-treated VP rabbits.

Early studies reported abnormal oral GTT results and hyperinsulinemia in patients with AIP,[43,46,47] which resemble the findings in cellular insulin resistance. More recently, we reported a high prevalence of insulin resistance and hyperinsulinemia in patients with AIP.[48] We also reported serum hyperinsulinemia, delayed GTT, and a different response to fasting between AIP and wild-type (WT) mice.[49] Glucose homeostasis in these fasted AIP mice was efficiently normalized after restoration of PBGD by gene therapy in the liver.[49] Altered GTT and reduced brain glucose uptake were also reproduced in our rabbit model, and only hPBGD mRNA administration efficiently restored both parameters. These data highlight that porphyrin precursor accumulation, but not porphyrins, are associated with altered glucose homeostasis.

In conclusion, recurrent AIA and rifampicin challenge in rabbits induced biochemical disturbances that were similar to those of severe VP in humans and reproduced some symptoms associated with acute porphyria attacks. The increase in *Alas1* expression can be explained by the combination of increased heme demand for hemoprotein function and a partial block in the synthesis pathway due to reduced PPOX activity. High accumulation of the early heme precursors upstream of the PBGD enzyme, mainly PBG, indicated that this is the limiting step in the liver of challenged rabbits. Of interest, i.v. administration of hPBGD mRNA improved mitochondrial hemoprotein functions and normalized hepatic *Alas1* induction as well as protein levels, indicating that PBGD, and not PPOX, was the critical enzyme for hepatic heme synthesis in VP rabbits.

Blood pressure and the function of important hepatic hemoproteins were closely associated with heme availability, while the accumulation of porphyrin precursors interfered with metabolic and physiological functions, such as glucose homeostasis, liver oxidative stress, motor coordination, and compound muscle action potential. Lipid peroxidation was closely associated with high ALA accumulations in rabbits challenged with AIA and rifampicin. Although most symptoms have been associated with high ALA accumulation,[50] this model also supports the involvement of PBG in the behavioral disturbances and pathophysiology associated with acute attacks.

MATERIALS AND METHODS

mRNA production and formulation

Codon-optimized mRNA encoding hPBGD was synthesized *in vitro* by T7 RNA polymerase-mediated transcription. The mRNA was initiated with a cap, followed by a 5′ untranslated region (UTR), an open reading frame (ORF) encoding hPBGD, a 3′ UTR, and a polyadenylated tail. Uridine was globally replaced with 1-methylpseudouridine. For *in vivo* i.v. delivery, LNP formulations were generated. Briefly, mRNA was mixed with lipids at a molar ratio of 3:1 (mRNA/lipid), with lipids composed of a molar ratio of 30:30:38.5:1.5 (ionizable cationic lipid/fusogenic lipid/structural lipid/PEG lipid). mRNA-loaded nanoparticles were exchanged into final storage buffer and had particle sizes of 80–100 nm, >80% encapsulation of the mRNA by a RiboGreen assay, and <10 endotoxin units (EU)/mL.

Chemically induced VP rabbit model

Thirteen female wild-type New Zealand rabbits (Granja de San Bernardo, Tulebras, Spain) were injected subcutaneously (s.c.) with 325 mg/kg AIA in the morning and 200 mg/kg (intraperitoneally [i.p.]) rifampicin in the afternoon. A total of 11 AIA and 12 rifampicin doses were administered during 20 days in three challenges, that is, days 1–3 (D1), D8, and D15. An additional dose of rifampicin was administered on day 20. Four rabbits were injected with four hemin doses of 8 mg/kg i.p. (Normosang, Recordati, Puteaux, France) from day 15 to 18, and three rabbits received a single dose of 0.5 mg/kg (i.v.) hPBGD mRNA on day 16. The hemin dose administered in rabbits is double the highest "standard dose" used in human acute porphyria patients (4 mg/kg). Given that i.p. administration of 8 mg/kg in mice reproduces the effects of i.v. hemin infusion in humans,[8,21] we used i.p. administration to preserve auditory pinna veins in the rabbits to carry out the GTTs and the administration of the hPBGD mRNA. Experimental protocols were approved by the Ethics Committee of the University of Navarra (CEEA142-16E1), according to European Council guidelines.

Biochemical and molecular parameters

24-h urine samples were collected daily over the three challenges. Urinary PBG and ALA levels were determined by ion-exchange chromatography (M11017c-0509, BioSystems, Barcelona, Spain) according to the manufacturer's instructions. Serum ALA and PBG were quantified by liquid chromatography-mass spectrometry (LC-MS) using a Waters XBridge BEH C18 column (2.5 μm, 2.1 × 50 mm). Calibration standards were prepared by adding diluted solutions of ALA (A3785-500MG), ALA-13C5 (711187, both from Sigma-Aldrich [now Merck], Darmstadt, Germany), PBG (P226-10MG, Frontier Scientific, Newark, NJ, USA), and C13-PBG (P41393, Inochem, Carnforth, UK) in acetonitrile/water (50:50, v/v) internal standard solution (100 μM) to blank serum. Standards were then purified using an OASIS PRiME HLB μElution plate (186008052, Waters Chromatography Europe, Etten-Leur, the Netherlands). The recoveries calculated for PBG and ALA in rabbit serum were between 88% and 98% and between 87% and 100%, respectively. ALA and PBG in the cerebrospinal fluid were measured by LC coupled to a triple-quadrupole MS system (Xevo TQMS, Waters, Milford, MA, USA), following a metabolite derivatization process (AccQTag, Waters, Milford, MA, USA).

Porphyrins were quantified in a PerkinElmer LS50B spectrofluorometer (excitation wavelength [λ_{ext}], 409; emission wavelength [λ_{em}] 600 nm; PerkinElmer, MA, USA) after oxidation with Lugol's iodine.[51] Total urinary porphyrins were determined by spectrophotometry (UV 1800, Shimadzu, Kyoto, Japan) between 350 and 450 nm after acidification, according to the method of Elder et al.[52] The different urinary porphyrins were separated by reverse-phase high-performance liquid chromatography (HPLC) with fluorometric detection (Ultimate 3000, Thermo Fisher Scientific, Waltham, MA, USA). Plasma porphyrins were measured by dilution of the plasma in phosphate buffer as already described.[53] The solution was compared with a standard by scanning the fluorescence emission signal from 570 to 750 nm (excitation at 405 nm), using a RF6000 spectrofluorometer (Shimadzu, Kyoto, Japan) fitted with a red-sensitive photomultiplier. Total fecal porphyrins were determined by spectrophotometry (UV 1800, Shimadzu, Kyoto, Japan) after hydrochloric acid extraction in the presence of ether.[54] The fractionation of fecal porphyrins was performed after formation of methyl ester porphyrins, which were then extracted with chloroform and finally separated by normal-phase HPLC with fluorometric detection.[55]

Lipid peroxidation was determined using the TBARS kit (Bio-Techne KGE013, R&D Systems, MN, USA) according to the manufacturer's instructions. Briefly, a colorimetric product formed by the reaction of malondialdehyde (end products of polyunsaturated lipids oxidation) with thiobarbituric acid was measured at λ of 532 nm in a Multiskan Ascent 96 plate reader photometer (Thermo LabSystems, CT, USA). Urinary parameter data were normalized per creatinine excretion rate. Creatinine levels were measured in a Cobas Hitachi c311 Analyzer (Roche Diagnostics International, Mannheim, Germany).

At sacrifice, rabbits were exsanguinated by intracardiac perfusion at room temperature before organ removal. Serum samples were stored at −20°C until analyzed. Liver status (ALT and ALP) was analyzed in a Cobas Hitachi c311 Analyzer (Roche Diagnostics International). PBGD activity was determined in each liver lobe by the conversion ratio of PBG to uroporphyrin in a PerkinElmer LS50B spectrofluorometer (PerkinElmer, MA, USA).[45] Liver tissue samples were also stored at −80°C for further analysis as follows: (1) Enzyme activities were determined in homogenates from a mix of liver lobes (ALAD as already described).[56] UROS III synthase activities were determined by an enzyme-coupled assay as described.[57] For UROD activity measurement, pentacarboxylporphyrinogen III was used as the substrate and its decarboxylation was quantified by HPLC as coproporphyrinogen III formation.[58] CPOX activities were determined as already described.[59] PPOX activities were quantified as described,[53] and FECH activities were measured fluorometrically by zinc-mesoporphyrin formation according to Li et al.[60] Activities of the respiratory chain were measured in isolated liver mitochondria according to previously described methods for spectrophotometric assays,[61] using

between 6 and 30 μg of mitochondrial protein. (2) Total heme levels were measured in liver homogenates using a heme assay kit (MAK316, Sigma-Aldrich, St. Louis, MO, USA). Mitochondrial heme *a* levels were measured using a colorimetric method. Briefly, 900 μg from isolated liver mitochondrial proteins were incubated on ice for 30 min with sodium phosphate buffer solution (23.8 mM final, pH 7.4) with 1.9% Triton X-100 (T9284, Sigma-Aldrich). Absorbance was measured at 445 nm in a Multiskan Ascent 96 plate reader photometer (Thermo LabSystems, CT, USA) at baseline (oxidized condition), and after adding 10 mg of ascorbic acid (reduced condition) (50-81-7, Sigma-Aldrich). Mitochondrial heme *a* levels were calculated by the absorbance increase between the reduced and oxidized condition taking into account the molar extinction coefficient (ε_{445nm}, 164 mM^{-1} cm^{-1}). (3) Gene expression was measured by real-time PCR with an iCycler IQ real-time PCR thermal cycler (170-8740, Bio-Rad, CA, USA) using iQ SYBR Green supermix (1708880, Bio-Rad, CA, USA). Briefly, mRNA was extracted from liver tissues using Maxwell RSC simplyRNA Tissue (Promega, Madison, WI, USA) and then converted into cDNA by reverse-transcriptase PCR (RT-PCR). qPCR was performed using specific primers for *Alas1* (sense, 5′-GCAGCAGTGTCGTCCGCAAA-3′; antisense, 5′- CGGAGAGGACCCCAGTGGAC-3′; product length, 141 bp); *Alad* (sense 5′-CTACCCCATCTTCGTCACGG-3′, antisense 5′-GCCTGGAATGCTCCGTTTTC-3′, product length: 333 bp), *Pbgd* (sense, 5′-AGCCCCAGGATGAGAGTGAT-3′; antisense, 5′- GCTGGTTCCCACTACACTCC-3′; product length, 396 bp), *Uros* (sense, 5′-GCCAGGATCCATACGTCAGG-3′; antisense, 5′-GCAGGCCGATTCTACTCACT-3′; product length, 294 bp), *Urod* (sense, 5′-GCCTGCTGTGAACTGACTCT-3′; antisense, 5′-ATGTCATCAGAGTCCACGGG-3′; product length, 301 bp), *Cpox* (sense, 5′-GTGGGAGAGGAAGGAAGGAG-3′; antisense, 5′-GGATAGTGGGAGCATGAGGA-3′; product length, 236 bp), *Ppox* (sense, 5′-TCTGGCTCGTGTCCTGAGTA-3′; antisense, 5′-TGGCTCCTTCAGTCCTAGCT-3′; product length, 316 bp), *Fech* (sense, 5′-AGCACTATTGACAGGTGGCC-3′, antisense, 5′-GCATGCGCACATACAGTCAG-3′, product length, 511 bp), *Ho*-1 (sense, 5′-AACCCGGTCTACGCCCCGCT-3′; antisense, 5′- CCATCCCCTACACGCCGGCC-3′; product length, 120 bp), *Hepcidin* (sense, 5′-GTTCTCCAGCAGCAGACACA-3′; antisense, 5′-TCAAAATGTGGGATCTGCTG-3′; product length, 170 bp), and *Hsp70* (sense 5′-TGGTGCTGACGAAGATGAAG-3′; antisense, 5′-AGGTCGAAGATGAGCACGTT-3′; product length, 235 bp). *β-actin* was used as control housekeeping gene (sense, 5′-CTGGAACGGTGAAGGTGACA-3′; antisense, 5′- AAAGTTCTGCAATGTGGCCG-3′; product length, 73 bp). Results are expressed according to the formula $2\Delta^{Ct(actin)-\Delta Ct(gene)}$, where ΔCt represents the difference in threshold cycle between the target and control genes. (4) For the western blot assay, liver samples were homogenized in radioimmunoprecipitation assay (RIPA) lysis buffer containing protease inhibitors and sodium orthovanadate and sonicated for protein extraction. 30 μg of protein was loaded for a room temperature electrophoresis procedure at constant 120 V in running buffer (192 mM glycine, 25 mM Tris, and 0.1% SDS). Then, separated proteins were transferred onto a nitrocellulose 0.45-μm or polyvinylidene fluoride (PVDF) membrane by a 4°C electrophoretic transfer at constant 120 V in a transfer buffer (192 mM glycine, 25 mM Tris, and 20% methanol). The primary antibodies used were as follows: anti-ALAS1 antibody (ab84962, dilution 1:750, Abcam, Cambridge, UK), total OXPHOS rodent western blot (WB) antibody cocktail (ab110413, dilution 1:500, Abcam, Cambridge, UK), and anti-actin antibody (A2066, dilution 1:4,000, Sigma-Aldrich). Anti-mouse (A0168, 1:10,000, Sigma-Aldrich) and anti-rabbit (7074, 1:10,000, Cell Signaling Technology, MA, USA) were used as secondary antibodies. Primary antibodies were incubated overnight at 4°C and secondary antibodies for 1 h at room temperature. Signals were detected using a Western Lightning Plus ECL kit (NEL103E001EA, PerkinElmer, MA, USA) in a ChemiDoc MP imaging system (Bio-Rad, CA, USA). Specific western blot signals for each OXPHOS complex were quantified with Imagen Lab software 6.01 (Bio-Rad, CA, USA) using actin protein for loading normalization.

Mitochondrial staining was performed in formalin-fixed liver sections using anti-mitochondrially encoded MT-CO1 (P00395, UniProt) (1D6E1A8, Abcam, Cambridge, UK) according to the manufacturer's instructions.

Physiological parameters

Blood pressure was measured at baseline (day −4) and on days 10 and 18, and the GTT was administered to fasted animals 1 day later. Blood pressure was determined by a non-invasive leg-cuff system in awake animals using a Hewlett-Packard M1165A model 56S apparatus. For the GTT assay, serum glucose levels (mg/dL) were measured at 0, 5, 10, 20, 30, 45, 60, 75, and 90 min post-injection of 0.5 g/kg (i.v.) of glucose solution (0.5 mg/mL) using a Accu-Chek AVIVA apparatus (Accu-Chek, Mannheim, Germany).

Brain and heart glucose uptake and electrophysiological studies were performed under inhaled isoflurane anesthesia at the end of the second and the third challenge (days 11 and 20, respectively). *In vivo* ^{18}F-FDG uptake in the brain was determined by positron PET after a fasting period of 16 h.[49] Rabbits were injected i.v. with 18.4 ± 0.1 MBq of ^{18}F-FDG. After a conscious uptake period of 45 min, animals were analyzed in a microPET (Philips Mosaic) tomograph (with 2-mm resolution, 11.9-cm axial field of view (FOV) and 12.8-cm transaxial FOV) (Cleveland, OH, USA), and a computed tomography Biograph Duo PET/CT (Siemens Healthineers, Knoxville, TN, USA).

Motor-evoked potentials in the sciatic nerve were recorded in anesthetized rabbits (0.3 mL/kg intramuscularly [i.m.] ketamine). The electrical stimuli were delivered using pairs of needles placed s.c. near the exit point of the sciatic nerve at the hip, with a separation of 0.5 mm and the cathode located distally. Stimuli were delivered by a Grass S180 stimulator (Grass-AstroMed, West Worwick, RI, USA). Motor potentials were recorded using steel needle electrodes (Viasys Healthcare, Lancaster, PA, USA) located at the center of the tibialis anterior muscle, midway between the ankle and the knee (active electrode), and at the dorsum of the foot (reference electrode). The responses were amplified by a Grass P511 amplifier (Grass-AstroMed), digitized using a CED power 1401 A/D converter

(Cambridge Electronic Design, Cambridge, UK), and stored in a PC using Signal 3 software (Cambridge Electronic Design). Stimulation intensity was increased gradually to ensure the maximal response amplitude. The largest response out of 10 biphasic negative-positive potentials was selected for analysis.

Statistical analysis

Statistical analyses were performed using GraphPad Prism v6.01 (GraphPad). Before statistical analysis, data were transformed using the formula log(1 + x) to normalize the variances. Comparisons between two groups were made by two-sided Student's t tests. In the case of comparisons between more than two groups, data were analyzed using a one- or two-way ANOVA, and pairwise comparisons were made using Bonferroni's multiple comparison tests. $p < 0.05$ was used to indicate statistically significant differences. Data are means ± standard deviation (SD). Confidence intervals were constructed as the normal-based 95% CI: mean ± 2 SD.

Availability of data and materials

The datasets supporting the conclusions of this article are included within the article and in the Supplemental information.

Web resource

National Institute of Diabetes and Digestive and Kidney Diseases, Bethesda, MD, USA. LiverTox: Clinical and research information on drug-induced liver injury. https://www.ncbi.nlm.nih.gov/books/NBK547852/.

SUPPLEMENTAL INFORMATION

Supplemental information can be found online at https://doi.org/10.1016/j.omtn.2021.05.010.

ACKNOWLEDGMENTS

The authors offer thanks for the technical and human support provided by the Central Service of Analysis de Alava (SGIker) of UPV/EHU. We thank N. Dessendier for technical assistance, and T. Lefebvre for help with the porphyrin precursor measurements in CSF. This work was supported in part by grants from the Spanish Institute of Health Carlos III (FIS) co-funded by the European Union (ERDF/ESF, "A Way to Make Europe"/"Investing in Your Future") (grant no. PI18/00860), the Spanish Fundación Mutua Madrileña de Investigación Médica, the Spanish Fundación Eugenio Rodríguez Pascual, and by the Spanish Fundación FEDER (Federación Española de Enfermedades Raras) para la Investigación de Enfermedades Raras [grant no. FI19010]. The financial sponsors had no role in the analysis or the development of conclusions. The investigators are solely responsible for the content and the decision to submit the manuscript for publication.

AUTHOR CONTRIBUTIONS

D.J., K.M.C., L.J., M.A.A, P.G.V.M., and A.F. designed the experiments. D.J., K.M.C., A.S., and A.F. performed the experiments and collected and processed animal samples and tissues. D.J., K.M.C., A.S., and A.F. completed behavior assays. M.A conducted the electrophysiological studies. C.C. performed the activity of the heme synthesis pathway enzymes, and K.M.C., A.S., and D.J. accomplished its fold change mRNA expression. K.M.C., A.S., D.J., and A.F. made blood pressure measurements. M.C. and I.P. performed PET studies. L.J. and P.G.V.M. designed and produced mRNA formulations, supervised mRNA production, and supported administrative, technical, and logistic tasks for sending and receiving samples. C.S., L.G., C.C., and A.F. performed the analysis and interpretation of the heme synthesis pathway and porphyria data. M.M., E.S.M., and M.A.M. accomplished mitochondrial function studies. A.E.-H.d.M. and J.O. designed the method and completed serum porphyrin precursor measurements. D.J., K.M.C., L.J., and A.F. performed all statistical analyses. D.J., K.M.C., L.J., C.S., E.A., M.A.A., L.G., P.G.V.M., and A.F. analyzed the data and wrote the manuscript, assisted by A.S. for figures and tables. All authors critically reviewed the manuscript for important intellectual content and gave final approval of the manuscript.

DECLARATION OF INTERESTS

L.J. and P.G.V.M. are employees of Moderna Inc., focusing on the development of therapeutic approaches for rare diseases. The remaining authors declare no competing interests.

REFERENCES

1. Puy, H., Gouya, L., and Deybach, J.-C. (2010). Porphyrias. Lancet *375*, 924–937.
2. Stein, P.E., Badminton, M.N., and Rees, D.C. (2017). Update review of the acute porphyrias. Br. J. Haematol. *176*, 527–538.
3. Bissell, D.M., Anderson, K.E., and Bonkovsky, H.L. (2017). Porphyria. N. Engl. J. Med. *377*, 862–872.
4. Stölzel, U., Doss, M.O., and Schuppan, D. (2019). Clinical guide and update on porphyrias. Gastroenterology *157*, 365–381.e4.
5. Junkins-Hopkins, J.M. (2010). Porphyrias. Clin. Pathol. Asp. Ski. Dis. Endocrine, Metab. Nutr. Depos. Dis. *375*, 83–90.
6. Podvinec, M., Handschin, C., Looser, R., and Meyer, U.A. (2004). Identification of the xenosensors regulating human 5-aminolevulinate synthase. Proc. Natl. Acad. Sci. USA *101*, 9127–9132.
7. Handschin, C., Lin, J., Rhee, J., Peyer, A.-K., Chin, S., Wu, P.-H., Meyer, U.A., and Spiegelman, B.M. (2005). Nutritional regulation of hepatic heme biosynthesis and porphyria through PGC-1α. Cell *122*, 505–515.
8. Schmitt, C., Lenglet, H., Yu, A., Delaby, C., Benecke, A., Lefebvre, T., Letteron, P., Paradis, V., Wahlin, S., Sandberg, S., et al. (2018). Recurrent attacks of acute hepatic porphyria: Major role of the chronic inflammatory response in the liver. J. Intern. Med. *284*, 78–91.
9. Yasuda, M., Erwin, A.L., Liu, L.U., Balwani, M., Chen, B., Kadirvel, S., Gan, L., Fiel, M.I., Gordon, R.E., Yu, C., et al. (2015). Liver transplantation for acute intermittent porphyria: Biochemical and pathologic studies of the explanted liver. Mol. Med. *21*, 487–495.
10. Drew, P.D., and Ades, I.Z. (1989). Regulation of the stability of chicken embryo liver δ-aminolevulinate synthase mRNA by hemin. Biochem. Biophys. Res. Commun. *162*, 102–107.
11. Lathrop, J.T., and Timko, M.P. (1993). Regulation by heme of mitochondrial protein transport through a conserved amino acid motif. Science *259*, 522–525.
12. Tian, Q., Li, T., Hou, W., Zheng, J., Schrum, L.W., and Bonkovsky, H.L. (2011). Lon peptidase 1 (LONP1)-dependent breakdown of mitochondrial 5-aminolevulinic acid synthase protein by heme in human liver cells. J. Biol. Chem. *286*, 26424–26430.
13. Fontanellas, A., Ávila, M.A., Anderson, K.E., and Deybach, J.-C. (2019). Current and innovative emerging therapies for porphyrias with hepatic involvement. J. Hepatol. *71*, 422–433.

14. Sardh, E., Harper, P., Balwani, M., Stein, P., Rees, D., Bissell, D.M., Desnick, R., Parker, C., Phillips, J., Bonkovsky, H.L., et al. (2019). Phase 1 trial of an RNA interference therapy for acute intermittent porphyria. N. Engl. J. Med. *380*, 549–558.

15. Balwani, M., Sardh, E., Ventura, P., Peiró, P.A., Rees, D.C., Stölzel, U., Bissell, D.M., Bonkovsky, H.L., Windyga, J., Anderson, K.E., et al.; ENVISION Investigators (2020). Phase 3 trial of RNAi therapeutic givosiran for acute intermittent porphyria. N. Engl. J. Med. *382*, 2289–2301.

16. Dowman, J.K., Gunson, B.K., Mirza, D.F., Bramhall, S.R., Badminton, M.N., and Newsome, P.N.; UK Liver Selection and Allocation Working Party (2012). Liver transplantation for acute intermittent porphyria is complicated by a high rate of hepatic artery thrombosis. Liver Transpl. *18*, 195–200.

17. Unzu, C., Sampedro, A., Mauleón, I., Vanrell, L., Dubrot, J., de Salamanca, R.E., González-Aseguinolaza, G., Melero, I., Prieto, J., and Fontanellas, A. (2010). Porphobilinogen deaminase over-expression in hepatocytes, but not in erythrocytes, prevents accumulation of toxic porphyrin precursors in a mouse model of acute intermittent porphyria. J. Hepatol. *52*, 417–424.

18. Medlock, A.E., Meissner, P.N., Davidson, B.P., Corrigall, A.V., and Dailey, H.A. (2002). A mouse model for South African (R59W) variegate porphyria: construction and initial characterization. Cell. Mol. Biol. *48*, 71–78.

19. Klinger, W., and Müller, D. (1980). The influence of allyl isopropyl acetamide on d-aminolevulinic acid synthetase and cytochrome P-450. Acta Biol. Med. Ger. *39*, 107–112.

20. McColl, K.E., Thompson, G.G., el Omar, E., Moore, M.R., Park, B.K., and Brodie, M.J. (1987). Effect of rifampicin on haem and bilirubin metabolism in man. Br. J. Clin. Pharmacol. *23*, 553–559.

21. Jiang, L., Berraondo, P., Jericó, D., Guey, L.T., Sampedro, A., Frassetto, A., Benenato, K.E., Burke, K., Santamaría, E., Alegre, M., et al. (2018). Systemic messenger RNA as an etiological treatment for acute intermittent porphyria. Nat. Med. *24*, 1899–1909.

22. Badminton, M.N., Whatley, S.D., and Aarsand, A.K. (2019). Porphyrins and porphyrias. In Tietz Fundamentals of Clinical Chemistry and Molecular Diagnostics, *Chapter 29*, N. Rifai, A.R. Horvath, and C.T. Wittwe, eds (Elsevier), pp. 524–540.

23. Atamna, H., Liu, J., and Ames, B.N. (2001). Heme deficiency selectively interrupts assembly of mitochondrial complex IV in human fibroblasts: Revelance to aging. J. Biol. Chem. *276*, 48410–48416.

24. Pigeon, C., Ilyin, G., Courselaud, B., Leroyer, P., Turlin, B., Brissot, P., and Loréal, O. (2001). A new mouse liver-specific gene, encoding a protein homologous to human antimicrobial peptide hepcidin, is overexpressed during iron overload. J. Biol. Chem. *276*, 7811–7819.

25. Pimentel, V.C., Pinheiro, F.V., Kaefer, M., Moresco, R.N., and Moretto, M.B. (2011). Assessment of uric acid and lipid peroxidation in serum and urine after hypoxia-ischemia neonatal in rats. Neurol. Sci. *32*, 59–65.

26. Masopust, D., Sivula, C.P., and Jameson, S.C. (2017). Of mice, dirty mice, and men: Using mice to understand human immunology. J. Immunol. *199*, 383–388.

27. De Matteis, F. (1971). Loss of haem in rat liver caused by the porphyrogenic agent 2-allyl-2-isopropylacetamide. Biochem. J. *124*, 767–777.

28. De Matteis, F. (1970). Rapid loss of cytochrome P-450 and haem caused in the liver microsomes by the porphyrogenic agent 2-allyl-2-isopropylacetamide. FEBS Lett. *6*, 343–345.

29. Bonkowsky, H.L., Healey, J.F., Sinclair, P.R., Mayer, Y.P., and Erny, R. (1980). Metabolism of hepatic haem and "green pigments" in rats given 2-allyl-2-isopropylacetamide and ferric citrate. A new model for hepatic haem turnover. Biochem. J. *188*, 289–295.

30. Bonkowsky, H., Sinclair, P., Healey, J., Sinclair, J., and Myer, Y. (1980). Kinetics of hepatic heme turnover in rats given allylisopropylacetylurea: A new model for liver heme catabolism. In Microsomes, Drug Oxidations and Chemical Carcinogenesis, *Vol. I*, M.J. Coon, A.H. Conney, R.W. Estabrook, V. Gelboim, J.R. Gillette, and P.J. O'Brien, eds. (Elsevier), pp. 571–574.

31. Nakamura, T., Okada, K., Nagata, K., and Yamazoe, Y. (2000). Intestinal cytochrome P450 and response to rifampicin in rabbits. Jpn. J. Pharmacol. *82*, 232–239.

32. Zuber, R., Anzenbacherová, E., and Anzenbacher, P. (2002). Cytochromes P450 and experimental models of drug metabolism. J. Cell. Mol. Med. *6*, 189–198.

33. Zanger, U.M., Turpeinen, M., Klein, K., and Schwab, M. (2008). Functional pharmacogenetics/genomics of human cytochromes P450 involved in drug biotransformation. Anal. Bioanal. Chem. *293*, 1093–1108.

34. Meissner, P., Adams, P., and Kirsch, R. (1993). Allosteric inhibition of human lymphoblast and purified porphobilinogen deaminase by protoporphyrinogen and coproporphyrinogen. A possible mechanism for the acute attack of variegate porphyria. J. Clin. Invest. *91*, 1436–1444.

35. Acocella, G. (1978). Clinical pharmacokinetics of rifampicin. Clin. Pharmacokinet. *3*, 108–127.

36. Faut, M., Paiz, A., San Martín de Viale, L.C., and Mazzetti, M.B. (2013). Alterations of the redox state, pentose pathway and glutathione metabolism in an acute porphyria model. Their impact on heme pathway. Exp. Biol. Med. (Maywood) *238*, 133–143.

37. Ferreira, G.C., Franco, R., Lloyd, S.G., Pereira, A.S., Moura, I., Moura, J.J., and Huynh, B.H. (1994). Mammalian ferrochelatase, a new addition to the metalloenzyme family. J. Biol. Chem. *269*, 7062–7065.

38. Homedan, C., Laafi, J., Schmitt, C., Gueguen, N., Lefebvre, T., Karim, Z., Desquiret-Dumas, V., Wetterwald, C., Deybach, J.C., Gouya, L., et al. (2014). Acute intermittent porphyria causes hepatic mitochondrial energetic failure in a mouse model. Int. J. Biochem. Cell Biol. *51*, 93–101.

39. Rötig, A., Sidi, D., Munnich, A., and Rustin, P. (2002). Molecular insights into Friedreich's ataxia and antioxidant-based therapies. Trends Mol. Med. *8*, 221–224.

40. Hermes-Lima, M., Castilho, R.F., Valle, V.G.R., Bechara, E.J.H., and Vercesi, A.E. (1992). Calcium-dependent mitochondrial oxidative damage promoted by 5-aminolevulinic acid. Biochim. Biophys. Acta *1180*, 201–206.

41. Lindberg, R.L.P., Martini, R., Baumgartner, M., Erne, B., Borg, J., Zielasek, J., Ricker, K., Steck, A., Toyka, K.V., and Meyer, U.A. (1999). Motor neuropathy in porphobilinogen deaminase-deficient mice imitates the peripheral neuropathy of human acute porphyria. J. Clin. Invest. *103*, 1127–1134.

42. Neeleman, R.A., Wagenmakers, M.A.E.M., Koole-Lesuis, R.H., Mijnhout, G.S., Wilson, J.H.P., Friesema, E.C.H., and Langendonk, J.G. (2018). Medical and financial burden of acute intermittent porphyria. J. Inherit. Metab. Dis. *41*, 809–817.

43. Tschudy, D.P., Valsamis, M., and Magnussen, C.R. (1975). Acute intermittent porphyria: clinical and selected research aspects. Ann. Intern. Med. *83*, 851–864.

44. Yasuda, M., Bishop, D.F., Fowkes, M., Cheng, S.H., Gan, L., and Desnick, R.J. (2010). AAV8-mediated gene therapy prevents induced biochemical attacks of acute intermittent porphyria and improves neuromotor function. Mol. Ther. *18*, 17–22.

45. Unzu, C., Sampedro, A., Mauleón, I., Alegre, M., Beattie, S.G., de Salamanca, R.E., Snapper, J., Twisk, J., Petry, H., González-Aseguinolaza, G., et al. (2011). Sustained enzymatic correction by rAAV-mediated liver gene therapy protects against induced motor neuropathy in acute porphyria mice. Mol. Ther. *19*, 243–250.

46. Sixel-Dietrich, F., Verspohl, F., and Doss, M. (1985). Hyperinsulinemia in acute intermittent porphyria. Horm. Metab. Res. *17*, 375–376.

47. Stein, J.A., and Tschudy, D.P. (1970). Acute intermittent porphyria. A clinical and biochemical study of 46 patients. Medicine (Baltimore) *49*, 1–16.

48. Solares, I., Izquierdo-Sánchez, L., Morales-Conejo, M., Jericó, D., Castelbón, F.J., Córdoba, K.M., Sampedro, A., Lumbreras, C., Moreno-Aliaga, M.J., Enríquez de Salamanca, R., et al. (2021). High prevalence of insulin resistance in asymptomatic patients with acute intermittent porphyria and liver-targeted insulin as a novel therapeutic approach. Biomedicines *9*, 255.

49. Collantes, M., Serrano-Mendioroz, I., Benito, M., Molinet-Dronda, F., Delgado, M., Vinaixa, M., Sampedro, A., Enríquez de Salamanca, R., Prieto, E., Pozo, M.A., et al. (2016). Glucose metabolism during fasting is altered in experimental porphobilinogen deaminase deficiency. Hum. Mol. Genet. *25*, 1318–1327.

50. Bissell, D.M., Lai, J.C., Meister, R.K., and Blanc, P.D. (2015). Role of delta-aminolevulinic acid in the symptoms of acute porphyria. Am. J. Med. *128*, 313–317.

51. Westerlund, J., Pudek, M., and Schreiber, W.E. (1988). A rapid and accurate spectrofluorometric method for quantification and screening of urinary porphyrins. Clin. Chem. *34*, 345–351.

52. Elder, G.H., Smith, S.G., and Smyth, S.J. (1990). Laboratory investigation of the porphyrias. Ann. Clin. Biochem. *27*, 395–412.

53. Da Silva, V., Simonin, S., Deybach, J.C., Puy, H., and Nordmann, Y. (1995). Variegate porphyria: Diagnostic value of fluorometric scanning of plasma porphyrins. Clin. Chim. Acta *238*, 163–168.

54. Lockwood, W.H., Poulos, V., Rossi, E., and Curnow, D.H. (1985). Rapid procedure for fecal porphyrin assay. Clin. Chem. *31*, 1163–1167.

55. Rossi, E., and Curnow, D.H. (1986). Porphyrins. In HPLC of Small Molecules: A Practical Approach, *Chapter 10*, C.K. Lim, ed (IRL Press), pp. 261–305.

56. Fujita, H., Orii, Y., and Sano, S. (1981). Evidence of increased synthesis of delta-aminolevulinic acid dehydratase in experimental lead-poisoned rats. Biochim. Biophys. Acta *678*, 39–50.

57. Tsai, S.F., Bishop, D.F., and Desnick, R.J. (1987). Coupled-enzyme and direct assays for uroporphyrinogen III synthase activity in human erythrocytes and cultured lymphoblasts. Enzymatic diagnosis of heterozygotes and homozygotes with congenital erythropoietic porphyria. Anal. Biochem. *166*, 120–133.

58. de Verneuil, H., Grandchamp, B., and Nordmann, Y. (1980). Some kinetic properties of human red cell uroporphyrinogen decarboxylase. Biochim. Biophys. Acta *611*, 174–186.

59. Lamoril, J., Martasek, P., Deybach, J.C., Da Silva, V., Grandchamp, B., and Nordmann, Y. (1995). A molecular defect in coproporphyrinogen oxidase gene causing harderoporphyria, a variant form of hereditary coproporphyria. Hum. Mol. Genet. *4*, 275–278.

60. Li, F.M., Lim, C.K., and Peters, T.J. (1987). An HPLC assay for rat liver ferrochelatase activity. Biomed. Chromatogr. *2*, 164–168.

61. Medja, F., Allouche, S., Frachon, P., Jardel, C., Malgat, M., Mousson de Camaret, B., Slama, A., Lunardi, J., Mazat, J.P., and Lombès, A. (2009). Development and implementation of standardized respiratory chain spectrophotometric assays for clinical diagnosis. Mitochondrion *9*, 331–339.